International Journal of Architectural Heritage
Conservation, Analysis, and Restoration

ISSN: 1558-3058 (Print) 1558-3066 (Online) Journal homepage: http://www.tandfonline.com/loi/uarc20

Structural characterisation and Numerical Modelling of Historic Quincha Walls

Natalie Quinn, Dina D'Ayala & Thierry Descamps

To cite this article: Natalie Quinn, Dina D'Ayala & Thierry Descamps (2015): Structural characterisation and Numerical Modelling of Historic Quincha Walls, International Journal of Architectural Heritage, DOI: 10.1080/15583058.2015.1113337

To link to this article: http://dx.doi.org/10.1080/15583058.2015.1113337

Article Title: Structural characterisation and Numerical Modelling of Historic Quincha Walls

Journal Name: International Journal of Architectural Heritage Conservation, Analysis, and Restoration

Corresponding Author: Natalie Quinn, n.quinn.12@ucl.ac.uk, PhD student, University College London, London

Co-authors:

Dina D'Ayala, d.d'ayala@ucl.ac.uk, Professor of Structural Engineering, University College London, London.

Thierry Descamps, Thierry.DESCAMPS@umons.ac.be, Department of Structural Mechanics, Faculty of Engineering - UMons , Mons, Belgium

Acknowledgements

The authors would like to greatly acknowledge the support of the SRP and all partners involved in the project. In particular, the authors would like to thank Daniel Torrealva and Erika Vicente from PUCP, and Claudia Cancino from the GCI for their input in the project. The authors are also grateful for the support of the European Commission FP1101 Cost Action.

Abstract

Quincha is a construction technique found in upper storeys of many historic residential buildings on the coast of Peru, consisting of a timber frame with a woven cane and mud infill. The paper presents the methodology for the development of a numerical model of the quincha system. The quincha walls have been subdivided into three components, the timber frame, bracing, and infill, and the modelling of each component is calibrated separately using experimental and analytical techniques. The resulting numerical model is found to successfully reproduce the behaviour of test specimens. The developed model can be used to assess the global seismic behaviour of

historic buildings containing quincha of varying geometries. This is demonstrated by modelling a portion of one of the facades of a well-known casona in Lima, Hotel el Comercio.

Introduction

Quincha is a construction technique found in historic buildings on the coast of Peru. It is comprised of a timber frame infilled with a weave of canes covered with mud and plaster. Although a rudimentary form of quincha was used prior to the arrival of the Spanish, the technique was developed and altered extensively between the 16th and 19th centuries. The technique reached its peak after the 1687 earthquake, when a law was passed ruling that quincha must be used for the upper storeys of any building greater than a single storey in height (Camilloni 2003). Today a number of these buildings survive, most dating from the 18th and 19th centuries, with quincha in the upper storeys, and the first storey in adobe or fired brick. However, many are in a state of deterioration and their numbers are dwindling.

This research is part of the Seismic Retrofitting Project (SRP), a collaboration between University College London (UCL), The Getty Conservation Institute (GCI), Pontificía Universidad Católica del Peru (PUCP) and the Ministry of Culture of Peru. The ultimate aim of the SRP is to determine a robust procedure to assess the seismic behaviour and design appropriate retrofitting systems for four case study buildings, selected because they are representative of typical historic construction typologies found in Peru (Cancino et al. 2012). The numerical models developed by UCL are based on nonlinear finite element analysis where both

material non linearity, mixed behaviour of the timber connections and irregular three dimensional geometry are considered.

The work reported in this paper focuses on the development of a robust strategy to model the structural components of a 19th century building in central Lima called Hotel el Comercio (HC) (Figure 1), representative of the Casona typology found in the coastal region of Peru. The advantage of studying this building is that it has already been the focus of some in-situ testing campaigns to obtain information on its dynamic properties (Cuadra et al. 2011, Aguilar et al. 2012).

Like other buildings from this time, the first storey of HC is constructed in adobe and fired brick masonry, while the upper two storeys are quincha (Figure 2). The composite nature of quincha, as well as the variability of the natural materials used, makes it difficult to develop a realistic model of the construction technique. Therefore, a thorough study has been carried out to develop numerical models of the quincha construction system, which can be used to create global numerical models of HC and other adobe-quincha buildings with minor modifications. This paper presents the methodology and outcomes of this study.

A typical quincha frame can be divided into three components, the vertical load bearing frame, the lateral bracing system, and the infill. The first component, the load-bearing frame consists of a series of vertical posts, connected at each end to horizontal beams by means of cylindrical mortice and tenon joints. The storey height can be up to 4.4m and the posts are typically spaced between 0.6 and 1.2m apart. For the second component, the lateral bracing, two distinct arrangements are present in HC. The first (Frame A), found on the second storey, is the use of

short diagonal struts to brace the lower portion of the frame as shown in Figure 3. Adobe blocks, or in some cases, small fired bricks, are placed in the space within the lower part of the frame to provide a modest increase in stiffness and to add weight to the frame. The second variation (Frame B), found on the third storey does not contain the struts or bricks, but has a large bracing member extending across several bays as shown in Figure 4.

The third component, the infill, consists of 25mm diameter horizontal canes passing through holes in the vertical posts. The canes are usually inserted through the posts in pairs, with four or five pairs evenly spaced vertically up the posts. Another set of tightly packed canes weaves vertically through them (Figure 5). A layer of mud mixed with straw is applied to the canes and covered with lime plaster.

Prior to the SRP initiative, little research had been published on historic quincha, with the only experimental work being on modern prefabricated quincha (SENCICO 2006, Miranda et al. 2000, Torrealva and Muñoz 1987). This differs substantially in geometry, construction method and in joinery techniques from historic quincha so the data is not directly applicable. Nevertheless, some of findings can be relevant. For example, Torrealva and Muñoz (1987) found from shaking table tests on a modern adobe-quincha specimen that almost all the stiffness of the structure arises from the walls acting in-plane, with almost no uptake of resistance from the out-of-plane walls. For this reason, the modelling of the quincha focuses on the in-plane behaviour while the out-of-plane behaviour is considered separately and is presented in a subsequent publication.

The lateral behaviour of quincha is difficult to predict since little published research is available on this construction technique, and the mechanical characteristics of the materials in the frames are variable and difficult to obtain. Therefore, each component of the composite structure (the vertical load bearing frame, the bracing, and the infill) is investigated in detail, in isolation and in combination with other components to determine the most significant parameters and their contribution to the overall structural behaviour. The scope is to develop an accurate finite element model of the two quincha systems (Frame A and Frame B), calibrated against experimental work, and then introduce simplifications which are necessary to build a model of the entire building, whilst still ensuring the model is representative.

This paper details the process of developing a numerical model of quincha using experimental work, numerical simulations and analytical techniques. First a general methodology for developing a detailed model of quincha is proposed; this entails identification of critical parameters from the observation and analysis of results of test campaigns conducted by the authors and the SRP partners. Such methodology is critiqued against current approaches available in literature. For each of the quincha components a detailed material characterisation is carried out highlighting the material parameters that are critical in determining its seismic response. Among these particular attention is paid to the modelling of the connections and the results obtained with the final model are compared to the experimental results. Finally a strategy for simplifying the detailed numerical model is proposed for use in global three-dimensional finite element models of real buildings.

Methodology

Quincha is a composite structural element made of non-engineered materials and components. Hence the process of developing a robust numerical model needs to take into account the lack of standardisation of the assembly while at the same time determine general rules for the interactions of the parts. The approach followed can be subdivided in three stages. The aim of the first stage is to obtain data on the geometry and material characteristics of the materials typically found in quincha walls. Where data cannot be obtained from literature, experimental tests are performed. The second stage consists of the development of a detailed numerical model of a section of a quincha wall, which is compared to experimental tests. The third stage involves a sensitivity analysis, resulting in simplification of the model for wider applications. The following section further explains this three-stage process.

In the first stage, which has been outlined in the flow chart in Figure 6, all the data required to develop the model is collated. As little literary reference exists, this is achieved mainly through direct on site survey of historic buildings, however, due to their historic significance, it is important to cause as little disturbance as possible to their historic fabric. Hence a balance needs to be found between the constraints posed by the preservation of their heritage value and the fact that the accuracy of a numerical model depends largely on the quality of the data on geometry and material characteristics obtained from on-site investigation. After an initial desktop study, preliminary elastic models of a section of a quincha wall are developed using geometry and material characteristics found in literature and from a broad observation of a number of sites (see Figure 6 Step 1). The commercially available finite element package Autodesk © Simulation

Multiphysics 2013 is used for analysis. Using the preliminary elastic models, a first sensitivity analysis is carried out varying the modelling approach, material characteristics, and connection stiffnesses as shown in Figure 6 Step 2, to establish which parameters have the most significant effect on the lateral behaviour of the frame. As a result, only the components found to be critical to the lateral stiffness are investigated in detail during the on-site data collection (Figure 6 Step 3), which in the case of the material characteristics or connection details enable minimal disturbance of the historic fabric. Material characterisation tests are then performed where necessary, and tests on components or connections are carried out to assess their behaviour (Figure 6 Step 4). Moreover, in order to verify the numerical models, in-plane laboratory tests are performed on replica quincha walls (Torrealva and Vicente 2012, Quinn and D'Ayala 2014) and, as the opportunity became available, on one quincha wall extracted from HC.

When all the required data has been obtained, the second stage, outlined in Figure 7, is to develop a detailed numerical model. The model is built up in components, comparing the outputs to the experimental results at each step before adding another layer of detail. Parameters, such as maximum displacement, elastic stiffness and uplift of the tenons are compared at each stage with those obtained experimentally. The inherent variability of the natural materials means that it is necessary to target a higher margin of error between experimental and modelled outputs than what could be achieved for steel or concrete models. Other numerical models on masonry infilled timber frames generally achieved a margin of error within 20% for pushover analysis compared with experimental results in terms of lateral stiffness and maximum force (Kouris and Kappos 2012, Ceccotti et al. 2006). Therefore this value has been selected as a target.

In the third, and final stage, a second sensitivity analysis is performed to identify and amend any limitation in the model, but also to simplify it by removing modelling details that do not significantly effect on the global behaviour. The simplified quincha model can then be successfully used to construct global models of entire buildings, such as HC, so their seismic response can be assessed within a reasonable computational burden.

In the following section we summarise the findings obtained by the experimental campaigns and how these informed the development of phase 2 of the analysis.

Experimental Work on Quincha Frames

Within the framework of the SRP, two sets of in-plane experimental tests on quincha frames were performed. These were informed by onsite surveys and carried out in parallel with the preliminary analysis.

To determine the stiffness, ultimate capacity and failure mechanisms of the separate components of quincha, the authors carried out a series of racking and push over to failure tests (Quinn, D'Ayala, and Moore 2012, Quinn and D'Ayala 2014). Specimens representing Frame A and Frame B (see Figure 3 and Figure 4) were tested with and without the infill of canes and mud, enabling the separate contribution of the infill and frame to be quantified (Figure 10 and Figure 11), and considering slightly different connection arrangements, as surveyed on site. Figure 8 and Figure 9 show the test setup of Frame A and Frame B respectively. The horizontal load was applied via a hydraulic jack connected to a 10kN load cell, while the vertical load was applied to a spreader beam on rollers through two hydraulic jacks. The testing program was based on the

procedure outlined in BS EN 594 (BSI 2011), with some modifications due to a differing geometry and lack of prior knowledge on quincha behaviour. Vertical loads of 6.4kN and 4.4kN were applied to Frame A and B respectively, representing the dead load of the floors and walls above. The lateral load was applied in three phases; Phase 1: a stabilising load cycle, Phase 2: a stiffness load cycle and Phase 3: a strength test. Phase 1 consisted of one cycle of 0.2kN, Phase 2 consisted of three cycles of 0.5kN, three of 0.7kN and three of 0.9kN, and in Phase 3 the frame was pushed to failure or 180mm, whichever occurred first. The load was applied at a rate of 40N per second, and maintained for 300s. Between each cycle the load was removed for 600s to allow the frame to settle.

A complementary set of in-plane cyclic tests was performed by PUCP, where a set of full scale replica quincha frames and one original frame extracted from HC were tested (Figure 12) (Torrealva and Vicente (2012). The lateral loading regime was cyclic and displacement controlled, consisting of four phases of ±25mm, ±50mm, ±100mm and ±140mm. A further phase of 300mm in one direction was applied for some of the frames. Each phase consisted of three cycles. Three variations in vertical load were considered for each frame, zero vertical load, half the estimated dead load, and full dead load so the influence of the vertical load could be determined. Safety factors were not applied. This is described in detail in Torrealva and Vicente (2012).

The major qualitative outcomes from all tests are summarised in Table 1, where modelling requirements are outlined as a direct consequence of observation and quantitative results from the tests. Furthermore, the decision taken for the modelling strategy identifies further testing of

local details and connections, which need to be pursued to fully calibrate the numerical model. It is seen that the infill has a fundamental role in stiffening Frame A, while in Frame B characterised by a full height timber diagonal member, the infill contribution is more modest. Cylindrical mortice and tenon connections are common to all post and beams forming both frames, however there is a large variation in diameter and length of the tenons as measured on site and the tests have shown that their translational and rotational stiffness differ depending on the tenon location within the frame. Further tests to determine these characteristics and how they are then simulated in the detailed model are discussed in section 6.1. For frame B substantial difference in behaviour was observed depending on the details of connection between the diagonal and the post or beam, this is further discussed in section 6.2.

Detailed Modelling Approach and choice of elements

A considerable amount of literature is available addressing the numerical modelling of bare timber framed structures covering a wide range of modelling approaches, which is comprehensively summarised by Mackerle (2005). Tsai and D'Ayala (2011) showed that it is possible to simulate the behaviour of historic timber frames by using linear elastic beam elements for the frame members coupled with nonlinear springs connecting them to represent the finite stiffness of the carpentry joints. The mechanical characteristics assigned to the springs are calibrated experimentally by testing real size joints, or using a detailed nonlinear numerical model. The resultant global models show a good correlation in terms of failure modes when compared to post-earthquake damage observations and experimental work. This technique is easy to implement in Autodesk Simulation, and decoupling the representation of the connections

from the members allows different carpentry joint types and their degrading behaviour to be represented without having to modify the entire frame.

Despite this, few studies have been published on the modelling of historic quincha frames, with the exception of two numerical models developed of HC. Paredes (2008) developed a global numerical model of HC to assess its seismic behaviour. The quincha walls were modelled using shell elements with the timber frame and infill homogenised, but no details are given as to how the mechanical characteristics of these homogenised elements were obtained. It is presumed that the model was not validated experimentally and estimated values were used. More recently, Aguilar et al. (2013) developed a linear elastic model of a section of HC for purposes of comparison with the results of experimental dynamic identification. The quincha walls were modelled using equivalent shell elements, the mechanical characteristics of which were found by developing more detailed solid models and determining characteristics from deflection equations. However, it seems likely that the mechanical characteristics were perhaps calibrated from the experimental results published by (Torrealva and Vicente 2012) as the mechanical characteristics of the homogenised quincha wall match perfectly with the initial stiffness obtained by the full scale tests of replica quincha frames. Although this model serves well as a comparison with the results of the dynamic identification, and can be valuable for obtaining the modal shapes of the building, it is impossible to extract localised stresses or strains. Furthermore, they cannot replicate post elastic behaviour, which has been shown experimentally to occur at relatively low values of lateral drift.

Although detailed numerical models have not been developed of quincha, a significant number of studies have be carried out on the modelling of other forms of traditional infilled timber construction. Many of these are infilled with masonry rather than mud and canes, and have additional timber cross bracing, or nailed connections, resulting in a substantially stiffer wall. Nonetheless, the techniques developed can be applicable to developing a model of quincha. When considering infilled timber frames the major difficulty is in determining the mechanical characteristics of the infill and its interaction with the frame. In certain types of infilled timber constructions such as the “Pombalino” or Dhajji-Dewari structural systems, it is common practice to neglect the infill, since in these cases some experimental data shows that the timber frame contributes the majority of the lateral stiffness and strength at failure (Ali et al. 2012, Cardoso, Lopes, and Bento 2005, Kouris and Kappos 2012). However, these structural systems differ substantially from quincha in that they all consist of a heavily cross-braced frame with nailed connections. Furthermore, Poletti, Vasconcelos, and Oliveira (2013) found through experimental work on “Pombalino” walls that the presence of the infill has a considerable influence on the stiffness, energy dissipation, ductility and failure modes of the timber frames.

The method of homogenising the timber and infill, and representing it using plate or volume elements, has also been used for “Pombalino” walls (Ramos and Lourenço 2004), and traditional masonry infilled Greek structures (Tsakanika - Theohari and Mouzakis 2010). The equivalent material properties were obtained experimentally (Ramos and Lourenço 2004) or through a detailed numerical model (Tsakanika - Theohari and Mouzakis 2010). In these cases, the method has been used to model entire structures to assess the global behaviour or effect of strengthening procedures. Although this technique is able to reproduce complex geometry and model entire

buildings, it cannot give a realistic stress distribution throughout the material so failure of timber elements or connections cannot be identified.

The most complex approach adopted in literature in terms of computational effort is to model the timber frame and the infill in detail using volume elements, taking into consideration all frictional contact between the infill and the frame as proposed by Hicyilmaz et al. (2012) for Dhajji-Dewari walls. The major issue with this approach is the resources required in terms of computational effort and time required to develop and run the model, and in the case of the quincha, this would still require a homogenisation of the mud and canes for the infill. It is therefore not suitable for the analysis of an entire structure. However, the detailed model can be used to validate a less complex model, which can then be used to assess a complete structure. Kouris and Kappos (2012) used this approach to develop simplified models of traditional masonry infilled walls found in Lefkas Island, Greece which were validated by more complex numerical models, in turn validated by experimental work on “Pombalino” walls. A less computationally demanding option is to use beam or truss elements to represent the timber frame, and plate or shell elements to represent the infill (Makarios and Demosthenous 2006). Timber connections may be considered as pinned, or assigned finite stiffness values using spring elements (Ferreira et al. 2014). The mechanical characteristics of the infill may be considered homogeneous, or an alternative strategy could be the use of composite layered elements, as available for instance in Autodesk Simulation Multiphysics (2013). However, to date there is no evidence of such uptake for these structures in literature. The normal and frictional contact between the infill and the frame may be included in the model by means of contact or interface elements, making it easy to alter the model complexity depending on requirements as

demonstrated by Pang and Shirazi (2010) for wood-frame shear walls. This strategy has been employed to model several types of masonry infilled structural systems including the "Pombalino" walls (Ferreira et al. 2014), and traditional Greek construction systems (Makarios and Demosthenous 2006, Doudoumis 2010, Karakostas et al. 2005, Doudoumis, Deligiannidou, and Kelesi 2005). The disadvantage of this approach is that it can be very computationally demanding, particularly if frictional contact between the frame and infill is considered. It can also be time consuming to develop the model depending on the capabilities of the software used.

A further simplification is to represent the stiffness provided by the infill using an equivalent brace or strut, as employed by Komatsu et al. (2009) for Japanese mud shear walls. This method is commonly used in the finite element modelling of masonry infilled frames (Chrysostomou, Gergely, and Abel 2002). The limitations of using such approach are discussed in D'Ayala, Worth, and Riddle (2009) and Ellul and D'Ayala (2012), in relation to determining the zone of interaction by contact as the deformation and degradation of the materials progress and in relation to overlooking critical failure modes. The mechanical properties and cross sectional area of the brace or strut must be calibrated on a case by case basis, either experimentally or with the use of a more detailed model. Similarly, Ceccotti et al. (2006) used a lumped plasticity approach to model traditional infilled frames from the Italian Dolomites. Linear elastic beam elements represent the timber frame, while inelastic hinges are used to represent the inelastic behaviour of the timber connections and the infill. The values assigned to the hinges are calibrated experimentally. Both these approaches can provide a useful insight into the global behaviour of the structure with a relatively low computational effort. However, local effects cannot be obtained from this model, and the bending moments and shear forces are not realistic as the

interaction between the infill and the frame is not modelled. In the case of the diagonal brace, it is necessary to consider carefully the location on the frame that the strut/brace is connected to, as it can cause localised stresses increases and unrealistic deformations in the frame. It is important to carry out a thorough sensitivity study when using this kind of model to ensure that small variations to one variable does not overly influence the global behaviour. Furthermore, in this instance, it is not possible to vary the geometrical or material characteristics of the frame, or to add openings without recalibration of the model.

In selecting the detailed modelling approach, a number of factors are considered. It is important that the model is not so refined that, due to the inherent geometric and material variability of historic structures, it would be necessary to re-calibrate the model for each and every geometric configuration. Furthermore, since adobe-quincha structures contain large openings, the modelling approach should be flexible enough to be able to easily adapt to real walls' configurations including openings. Preliminary models were used to assess the most suitable approach by varying parameters such as element type, material model, boundary conditions and method of reproducing the experimental loading conditions. As shown in Figure 6, part of the parametric analysis involves investigating the modelling approach. One such case investigated was the option of modelling the quincha wall using shell elements with homogenised material characteristics determined by fitting the pushover curve of the model to that obtained from experimental tests on quincha walls. The problem with this approach is that it does not allow for making minor modifications in geometry to take into account variations such as the presence of openings or minor changes in the cross section of the timber elements, without performing further full-scale experimental tests to recalibrate the model. Furthermore, the model did not

show realistic deformations under vertical loading. Therefore, a model consisting of separate timber and infill elements is considered to be more realistic and adaptable to changes in the structure. Overall, the most appropriate approach is considered to be modelling the timber frame using beam elements, with the infill modelled with plate/shell elements. The model can then be made more or less complex, as required, by considering or neglecting connections' finite stiffness, inelastic behaviour of the frame, and contact between the frame and the infill.

The experimental tests showed that both the bare timber frame and the infilled frame have inelastic behaviour. In the case of the timber frame, this mainly arises from relative movement at the connections and yielding or crushing of the fibres when approaching failure, while for the infill this is due to early cracking in the mud, at a relatively low displacement, and detachment of the mud from the cane at a larger displacement demand. To reproduce these observations in the detailed numerical model: the vertical and horizontal timber elements are modelled as isotropic using linear elastic beam elements; the mortice and tenon connections are modelled as semi-rigid with a finite rotational and translational stiffness. The top connections are modelled by simulating continuity between the beam and the post as far as vertical translation is concerned, while the rotational stiffness is simulated with a beam element with an equivalent bilinear Von Mises material model for the rotation. The Von Mises material model enables plastic deformation, and the bilinear stress-strain relationship is obtained from experimental tests on replica joints, discussed in section 6.2. The bottom connections are simulated by using a truss element with a high compressive stiffness and a low tensile stiffness, which allows for vertically upwards relative movement between the post and the beam, in this way simulating the uplift of the tenon. These choices, including the experimental testing, were developed based on

requirements determined as a result of the preliminary analysis. The whole process is detailed in Figure 7.

For Frame B, the initial sensitivity analysis showed an order of magnitude difference in lateral drift response depending on the type of element (truss or beam) chosen to simulate the diagonal member. The test of the bare frame confirmed that the best choice was the use of beam elements, because as the global deformation increases or when the diagonal is put in compression, in cyclic loading, the rotational and shear stiffness of the diagonal is activated due to the presence of half lap joint with the posts. The connection between the diagonal and the top and bottom beams is simulated using a nonlinear truss element with stiffness and capacity calculated depending on the geometry and material of the two timbers and the type and arrangement of nails, as discussed in section 6.2.

Although the infill of cane and mud is in itself an orthotropic composite material, it is considered most effective to model it as an equivalent homogeneous isotropic material using a Von Mises material model with isotropic hardening. The equivalent constitutive law is obtained by performing shear tests on small panels of mud and cane as discussed in section 5.2. The interaction between the frame and the infill is modelled using compression-only contact elements, as general surface contact cannot be used with the choice of finite element made for the timber and infill. The compression modulus of the contact element is calculated from the modulus of elasticity of the timber perpendicular to the grain obtained from experimental tests or literature. The addition of contact elements significantly increases the run time of the model so it is important to determine the extent of the surfaces in contact during the loading and unloading.

This is achieved by running a model with all possible contact simulated representing the tests and then eliminating the inactive contact portions, as a result of the model calibration. These simplified models are then used in the simulation of the full structure as describe in detail in section 8.

The test of the frame without infill showed that the horizontal canes are critical to the behaviour of the frames as they provide some additional lateral bracing. To simulate this contribution the canes were modelled using beam elements with contact elements between the canes and posts to simulate their ability to slide horizontally through the holes in the posts. The contact elements had no tensile capacity and a compressive stiffness equivalent to the stiffness of the timber in the post.

Materials, Characterisation and simulation

Use of parametric analysis to determine test needs

As described in the introduction, quincha contains timber, adobe, canes and mud. In order to develop a robust model, it is important to know the mechanical characteristics of these materials. According to Camilloni (2003) and Walker (2008), as far as timber is concerned the species most commonly used for quincha in Lima in the viceroyalty period was Spanish cedar (cedrela odorata) (which is actually not a true cedar, but more closely related to true mahoganies (Meier 2014)) or oak (quercus). These woods were resistant to insect attack and typically imported from Ecuador or Central America (Camilloni 2003). However these two materials have very different

mechanical characteristics, as the oak is more dense than the Spanish cedar (around 640kg/m^3 compared with 470kg/m^2), and has a higher elastic modulus in bending (20.8GPa compared to 10.3GPa) (Bergman et al. 2010). The assumption of either of them being the constitutive material of the timber frames in HC would lead to substantially different structural behaviour so it is necessary to properly characterise the materials found on site. In order to minimise extraction of historic material for the purpose of laboratory destructive testing, a parametric analysis is conducted to restrict the number of material parameters that require characterisation. The effect of variation in the timber elastic modulus, Poisson ratio and density were investigated in the parametric analysis using the range of values found in literature. It was established that the analysis was most sensitive to variations in the elastic modulus in bending, as small variations of this parameter cause the greatest effect on the lateral drift. Accurate determination of this value is crucial as a difference of 30% in drift was computed by assuming the minimum and maximum value of elastic modulus provided by literature. This variation is further increased if the rotational stiffness of the connections is low.

The adobe or masonry used at the base of the second floor frame is likely to vary substantially from building to building depending on workmanship and age of the structure. The mechanical characteristics of existing adobe in Peru, mainly in Lima, but also in Cusco, are better researched than timber (Ruíz et al. 2013, Tarque 2008, Blondet and Vargas 1978, Vargas and Ottazzi 1981, Vargas 1980, Rojas-Bravo and Fernandez Baca 2012). This enables a realistic range of values to be obtained, but it was shown in the preliminary tests and in the parametric analysis that the effect of the adobe is mainly as stabilising load, contributing little to overall stiffness and strength. Hence the only parameter of relevance for this analysis is its specific weight. On the

other hand variations in the characteristics of the composite infill had a significant effect on the lateral behaviour of the frame, particularly the characteristics in shear. The extraction of undisturbed samples of mud from the site for a full mechanical characterisation is a difficult undertaking. However some of the material can be extracted to determine its granulometric composition and plastic limits, after which a similar mixture can be reproduced in the laboratory and used in tests of the infill composite to determine its shear strength.

According to Cuadra et al. (2011), the canes are typically very thin and of the species caña brava or carrizo. Some information on the mechanical characteristics of these canes in Peru has been published by Barrionuevo (2011). The canes are not observed to undergo any progressive damage either in the bare frame or in the infilled frame. However as already mentioned, the horizontal ones contribute to the stiffness of the bare frame and both sets contribute to the stiffness of the infill.

Material Testing

Visual grading of the timber was impaired by the fact that most of the timber elements are concealed by original mud and lime plaster. The few exposed timber elements were found in a higher state of decay than the ones concealed by plaster, perhaps due to the high humidity levels, so visual grading of the exposed timber could be misleading. In order to obtain more conclusive data as required based on the outcomes of the preliminary analysis, a full characterisation of the timber in HC was performed by Custodio, Mallque, and Delgado (2012) complying with ASTM D143-94 (2007). The species of representative structural elements in the frames were determined, and samples were tested to quantify density, elastic moduli and compressive strength

for each species. The wood had an average humidity of 17.3% but it was not suffering substantial deterioration from insect infestation (Custodio, Mallque, and Delgado 2012). Frame A was found to contain two species; sapele, also known as caoba Africana (Entandrophagma cylindricum), for the beams, and cypress (cupressus) for the posts and citara struts, as shown in Figure 13. Frame B, shown in Figure 14, contains sapele in the bottom beam and cypress for the remainder of the frame.

Sapele is a wood originating from Africa, and is a member of the same family as 'true mahogany' (Swietenia Macrophylla) which originates from Central America and was widely forested across Latin America including Peru in the 18th and 19th centuries (Lamb 1947). Both woods are similar in appearance and properties to Spanish cedar, reported to have been typically used in quincha (Camilloni 2003, Walker 2008). Cypress is a name given to a many species of tree within the Cypressus family, and thus the precise species or geographical origin of the wood in HC is uncertain. For comparison of mechanical characteristics, the data from the species originating from Northern and Central America has been used, simply due to geographical proximity. Characteristic values for the mechanical properties of all three woods as reported by Bergman et al. (2010) and Meier (2014) who obtained the data from literature are presented in Table 2. These are compared with the values provided by Custodio, Mallque, and Delgado (2012) obtained by testing wood samples extracted from HC. The mechanical characteristics of the specimens extracted from HC are for both species substantially lower than the reference values found in literature, which is to be expected considering the reference values are for unweathered timber. However no statistical distribution is provided for the test results, so it is difficult to comment on their representativeness. Additionally, the environmental humidity in

Lima is high, and the moisture content, which substantially affects the strength properties of wood, was found to vary significantly with values of between 14.2% and 24.0% being recorded in different locations of the building. For the purpose of numerical modelling, the mechanical characteristics given by the experimental tests are used.

The racking tests demonstrated clearly the contribution of the infill for resisting lateral loads. From the initial sensitivity analysis, the characteristics of the infill were found to be very significant, in particular, the shear modulus. As detailed in the methodology, it is difficult to obtain accurate mechanical characteristics for the infill material due to its composite nature, and its interaction with the timber frame. Examples of experimental work to determine the shear stiffness of this type of panels are González and Gutiérrez (2005) and Komatsu et al. (2009), but they do not decouple the frame from the infill and hence they cannot be used as reference for the present mud cane composite. To obviate this gap, small sections of the infill in isolation were tested to determine mechanical characteristics in compression and shear. However, the difficulty in replicating the boundary conditions of the infill while confined in the timber frame rendered these test results unreliable. Therefore, a calibration was performed using the results from the tests of Frame A with and without infill, and the corresponding models. In this calibration, the shear characteristics of the infill in the model were increased until the model closely reproduced the experimental results of the infilled frame, within the set error margin. This was appropriate since the model of the bare frame correlates well with the experimental results, and the only difference between the bare frame and the infilled frame is the addition of the infill. All other parameters were kept constant. Figure 15 compares the results obtained for three variations of material properties with the experimental results. By trial and error, varying the material

characteristics of the infill only, it was found that Model A most closely aligns with the experimental curve. Therefore, the values in Model A were used for all other models. The shear characteristics of the infill obtained by this process are detailed in Table 3 and used in all other models. The properties of the contact elements were not included in the calibration procedure since they were obtained directly from spring equations based on the mechanical properties of the timber.

Table 3 summarises the mechanical characteristics used in the numerical models. The most significant parameters according to the results of the preliminary analysis, such as the elastic modulus of the timber, were obtained experimentally, while the less critical values, such as the adobe elastic modulus, are taken from literature. The preliminary analysis found the mechanical characteristics of the horizontal canes to be less significant to the composite behaviour. There is little experimental data available in literature for this species of canes since they are not normally used as structural elements. Therefore, similar sized canes were tested to obtain reasonable estimates for density and elastic modulus. For the timber, the characteristics of the two main species identified on site are used, as described in Section 5.2. The timber, adobe and canes are all modelled as isotropic, with the nonlinear behaviour in the case of the timber and horizontal canes being confined to the connections. The infill of canes and mud is modelled as a homogenised shell element with a material bilinear constitutive law and a Von Mises failure domain with isotropic hardening.

Characteristics of the Connections

Three types of timber connection can be observed in the quincha frames in HC. The first is the mortice and tenon joint connecting the vertical and horizontal components. The tenon is cylindrical and passes through the mortices without any dowel or nails to provide tensile capacity (see Figure 16). The second type is the nailed connection that connects the citara to the vertical posts (Figure 17) and is only found in Frame A. The third type is only found in Frame B and connects the diagonal brace to the frame (Figure 18). The diagonal is connected to the beam by a lap joint, where the beam has been cut away to a depth of half the thickness of the diagonal, although the diagonal itself retains its full cross section. The stiffness of the nailed connection between the citara in the posts in Frame A was found to be of low significance to the lateral behaviour and as such was not considered in detail individually. Therefore, only the connection characteristics of the mortice and tenon joint and the diagonal brace connection were considered fully.

Mortice and Tenon Connection

Rotational Stiffness

Preliminary analyses of the two frames with the commonly accepted assumption that all mortice and tenon joints could be considered as simply pinned resulted in lateral displacements twice as large as the experimental ones. This indicates that the pinned assumption is simplistic. In addition, it was observed during tests, that the mortice and tenon connections clearly possess

some rotational stiffness confirmed by observed yielding and rupturing of the tenons. Therefore to improve the accuracy of the timber frame numerical model, the connections are simulated as semi-rigid, with a finite rotational stiffness.

On-site investigations showed that there is a wide variation in geometry of mortice and tenons within HC. Figure 19 depicts the variation in length and diameter of tenons measured onsite. The noticeable differences, particularly in length will significantly affect the rotational stiffness calculated. For Frame A, this is more significant for the top tenons since the bottom tenons are offered some restraint by the citara, and adobe blockwork. It can be seen in Figure 19 that the length and diameter of the top tenons of Frame A vary substantially. In order to quantify this effect, a parametric analysis was carried out using a numerical model based on the geometry of Frame A, in which only the rotational stiffness of the top tenons were varied. This showed that the model is very sensitive to variation of the rotational stiffness up to 20kNm/rad, beyond which, any additional increase in stiffness has little effect on the overall model lateral stiffness (see Figure 20).

Therefore it is necessary to find a way to determine the rotational stiffness based on the geometrical properties of the joint so that a relationship between geometry and rotational stiffness can be obtained. One such analytical technique for doing this is the component method, which has been widely used to determine the rotational stiffness of mortice and tenons carpentry joint in European roofs (Drdacky, Wald, and Mares 1999, Wald et al. 2000, Descamps, Lambion, and Laplume 2006). The component method divides the joint into a number of components, one for each pair of surfaces in contact. The stiffness of each component is represented by a series of

springs, which combine to give the overall stiffness of the joint. The major issue with this method is that it assumes that the centre of rotation (C.O.R.) of the joint is located at the centre of the tenon, which is not realistic in the present case, as the lack of a dowel allows the tenon to pull out of the mortice when loaded laterally. To tailor the model to the specific problem, an assessment was carried out to identify a more realistic location for the centre of rotation based on experimental testing. The component method was then modified once the surfaces in contact were identified and the centre of rotation accurately located.

Two tests were performed on joints similar to those observed in HC. Although both joints were cut to the same dimensions, one of the joints had a very tight fit between the mortice and tenon and had to be hammered into the mortice, while the other was just and could easily be slotted into place. For ease of manufacturing, the tenons were square rather than round; the posts were 60mm square, while the tenons were 25mm square and 50mm in length. This makes this joint half-scale compared to the top tenons of Frame A found onsite in HC (see Figure 19). The post was pushed horizontally inducing a moment, until failure. The moment-rotation curve for the two tests is shown in Figure 21. The initial rotational stiffness of the joint was found to be 8.1kNm/rad for the tight fit and 2.6kNm/rad for the just fit. The ultimate load was 0.37kNm for the tight fit joint and 0.25kNm for the just fit joint as defined by BS EN 12512:2001 (BSI 2001), meaning that the tight fit joint is around 40% stronger, and about three times stiffer. It is worth noting that square mortice and tenon joints could have a capacity of between 11-17% lower than that of a round tenon (Sparkes 1968).

By considering the test results, a better estimate for the centre of rotation can be obtained. Figure 22 shows the test specimen at the point of yield. By inspection it can be seen that the C.O.R. is located somewhere to the right hand side of the tenon. By drawing perpendicular bisectors (in blue) on the photograph between the original location (outlined in red) and the location after rotation (shown in black), it can be found that the C.O.R. at this point of the test is located close to the region marked by a circle in Figure 22. A small level of translation towards the centre of rotation also occurs, which can be observed in the corner of the post directly above the centre of rotation. To verify this, three different assumptions for the C.O.R. were considered; the centre of the tenon (A), the edge of the shoulder (B), and half way through the depth of the beam directly below the edge of the shoulder (C) (see Figure 23). The location that produced a value for rotational stiffness closest to the experimental result was the third assumption, located on the axis of the beam directly below the edge of the shoulder. This actually simplifies the calculation, due to the fact that only the two portions of the tenon directly in contact with the walls of the mortice contribute to the stiffness as indicated in Figure 24. The stiffness provided by the contact between the shoulder and the beam can be considered negligible. This lack of contribution from the shoulder explains the overestimated value of stiffness obtained when applying the component method in its typical format (case A of Figure 23).

Using this modified method it was possible to determine more realistic estimates for rotational stiffness and as a result obtain a relationship between the length of the tenon and the rotational stiffness, which is shown in Figure 25. As discussed previously (see Figure 20) the parametric analysis showed that there is a large variation in the overall lateral stiffness of the frame for joint rotational stiffnesses of the top joints lower than 20kNm/rad, so it is important to accurately

correlate length and stiffness for values lower than this. As the length of the tenon is the most significant parameter (as this is related to the length of the lever arm), the length at which the stiffness is less than 20kNm/rad can be determined to be 70mm from Figure 25. This reduces the number of joints that need to be considered individually.

Figure 26 illustrates how the rotational stiffness decreases as the tenon uplifts out of the mortice for the configuration of the bottom tenons of the original quincha wall. The largest vertical uplift measured during the test on the historic quincha frame was 24mm, corresponding to a rotational stiffness of 11kNm/rad. This value is greater than what was found during the joint only test as it is for full scale geometry as opposed to half-scale. However, the parametric analysis found that a decrease in rotational stiffness is less significant for the bottom tenons than the top due to the presence of the bracing. For these reasons, the bottom tenons are assigned a constant value in rotational stiffness of 11kNm/rad which is the lower bound value shown in Figure 26. Moreover test observations proved that only the bottom tenons lift out of the mortices due to the applied vertical load. Hence the original stiffness for zero uplift is applied to the top tenons.

Translational Stiffness

Since there is no dowel to give tensile capacity to the mortice and tenon joint, a defining feature of the frames is the ability of the posts to move upwards. Ignoring this fact, and assuming that the connection has tensile capacity simplifies the model. However, increased stresses are observed in the posts and the overall lateral deflection is up to four times smaller than if the post is allowed to move upwards with some level of stiffness. This increased lateral deformation is

the combined result of lower lateral bending stiffness and rigid rotation movement around the leeward bottom tenon which results in uplift of the other tenons.

To model this, a nonlinear truss element is used with a compressive stiffness equal to that of the two wood members in contact, while any tensile resistance is only due to the friction between the mortice and the tenon. The amount of resistance will vary significantly depending on whether there is a loose or tight fit, which cannot be determined for every case. The resistance is also related to the rotation of the joint, as more rotation increases the frictional resistance, but when the tenon has already started to pull out such frictional resistance will reduce. To include this complex mechanical behaviour in a model would require a further set of thorough localised tests which were not included in the first campaign. Therefore the varying tensile stiffness is calibrated from the experimental data of vertical uplift measured for each relevant frame.

Diagonal Brace Connection (Frame B)

In all tests, failure occurred in the diagonal connection (see Figure 27). Due to the greater depth of the top beam as opposed to the tested ones, as later observed on site, it is thought that the connections of the on-site frames are slightly stronger than the ones tested in the laboratory. Assuming that the timber members are all in good condition, test results show that the most likely failure mode involves the diagonal moving downwards along the groove in the top beam, and yielding of the nails as shown in Figure 28. Negligible rotation of the diagonal with respect to the top beam was observed so the connection can be assumed to be flexurally rigid, with only the ability to move axially.

Factors affecting the behaviour of nailed joints include the mechanical properties of the wood, the material and geometry of the nail, the direction of the grain, and number of nails and their spacing, and the type and duration of loading (EN 1995-1-1 2005). These parameters vary from one connection to another. Therefore, as with the mortice and tenon joint, an analytical method is required to calculate the stiffness and capacity of the connection for small variations of the above parameters without the need for experimental calibration on a case-by-case basis. Furthermore, due to the vernacular nature of the structural system, the capacity of the joints is more difficult to predict since the carpentry techniques and workmanship is variable.

A wide range of empirical models have been developed to obtain load-deformation relationships for nailed timber connections, many of which have been summarised by Ramskill (2002). Many of these methods have accurately predicted the behaviour of a specific type of connection, but it is questionable whether they can be applied directly to the specific joint found in quincha walls without experimental calibration. This is particularly true if the model is to be used for all variations in geometry found. A simplified theoretical equation for the load-slip behaviour of a nailed timber joint was proposed by Wilkinson (1971):

$$P=0.1667[\![E]\!]^{(1/4)} [\![(K_e)]\!]^{(3/4)} d^{(7/4)} \delta \qquad (1)$$

where P = lateral load (lb.) at slip δ (inch); d = diameter of the nail (inch); E = modulus of elasticity of the nail (psi); Ke = elastic bearing constant (lb./in3), where the Ke = 3,200,000 (SG) and SG is the specific gravity of the wood.

As with many early models, the nail was assumed as a beam on an elastic foundation. When the elastic stiffness of the connection was calculated using this equation, and used in the numerical models, the models showed good agreement with experimental results in terms of initial lateral stiffness. The connection capacity was calculated according to the approach outlined in Section 6.3 of EN 1995-1-1 (2005) for single shear connections. The load-deformation behaviour of the connection was simplified as bilinear.

Comparison between Numerical and Experimental Results

The following section compares the results from the numerical models of frame A and B with those from the experimental tests. This was done for all test specimens from Bath and PUCP with and without infill. The pushover curves from the numerical models are compared with the pushover curves from the experimental results. The deformed shapes are shown for comparison. All models were analysed in force control rather than displacement control as the facility for displacement control is not available in Autodesk Simulation Multiphysics (2013) when spring elements are used. The analysis was terminated when the maximum force attained in the experiment was reached. As detailed in section 2, and shown in the flowcharts in Figure 6 and Figure 7, the models were first calibrated using the experimental tests of the half scale frames. The mechanical properties are shown in Table 3. When the results were found to be within the margin of error of 20%, the same approach was then taken for the full scale test specimens, which were analysed under cyclic loading.

Numerical Simulation of Racking Tests on Half-Scale Frames

Frame A

The numerical models of Frame A showed very good agreement with the experimental results with a variance of less than 10% in terms of initial stiffness, maximum capacity, and residual drift. The deformed shape of the bare frame numerical model is shown in Figure 29 (before the top mortice and tenon joints had yielded) and Figure 30 (after the top mortice and tenon joints had yielded). The experimental frame at 100mm displacement is shown in Figure 31 where it can be seen that the top mortice and tenon joints are providing little rotational resistance, similarly to the model in Figure 30. The model of the infilled Frame A is shown in Figure 33 alongside a photograph taken during the test at the same lateral displacement (Figure 32).

The pushover curves of the bare frame and the infilled frame are shown in Figure 34 and Figure 35 respectively. The initial stiffness of both models have a variance of less than 3%, and for both models yielding occurs at the same lateral displacement. Additionally, the model of the bare frame reproduces the residual deformation of the frame well, with only a variance between the model and test results of 6.5%. Based on the close approximation of the model to the experimental results it is concluded that the modelling process is reliable and the same process can be applied to the full scale frames.

Frame B

The numerical model of Frame B without infill is shown in Figure 36 alongside the test specimen in Figure 37, while Figure 38 and Figure 39 compare the model and test specimen for the infilled frame. The models has a good agreement with the tests in terms of deformed shape with the exception that the post on the opposite side to where the load is applied has more bending at the bottom of the post, as it appears that the experimental frame has less rotational stiffness in the joint than the model.

Figure 40 and Figure 41 show the pushover curve for the experimental test on Frame B with that obtained from numerical analysis for the bare frame and infilled frame respectively. When the diagonal is in tension, results are shown within the linear range since propensity for buckling was not included in the model, and the experimental test specimen failed in buckling. The results of the model in compression correlates well with the test results up to this point, indicating that for smaller deflections, the use of the nonlinear truss described in section 6.2 to represent the connections of the diagonal is sufficiently robust, considering that buckling was not observed at any stage of the testing of fully infilled frames, as would be found on site. Additionally, the stiffness and capacity of the infilled model are within a margin of error of less than 5% when compared to the test data.

Numerical Simulation of Cyclic Tests on Full-Scale Frames

The models of the half scale tests show a very good agreement with the experimental results, with a margin of error of less than 5% for initial stiffness and the capacity. However, in order to

be determine whether the models can replicate cyclic loading, further numerical models are developed of the frames tested by Torrealva and Vicente (2012) using the same process, but without the additional calibration of the bare frame tests.

Frame A

Figure 42 compares the deformed shape of the experimental frame with the modelled frame in Figure 43. The cyclic curves of the model and experimental results are shown in Figure 44. The model does not achieve the initial high stiffness of the test frame nor the subsequent softening. The first cycle of the test frame reaches a displacement of 25mm at a load of 5.5kN, whereas the model shows a 50mm displacement at the same load. Although the model shows a small reduction in capacity, it is not as pronounced as the experimental frame. Despite this, the deformed shapes are similar, and the stiffness is comparable for the 50mm and 100mm cycles.

Table 4 compares the lateral load obtained by the test and the model for different lateral displacements. The first cycle of 50mm in the model is compared with the second cycle of the same displacement in the tests, although this significant simplification neglects the initial high stiffness of the test frame. It can be seen that for the majority of the displacements recorded, the lateral load obtained by the model is well within the 20% error targeted. However, at the higher cycles of 100mm displacement, the model has a stiffer response than the experimental frame, as there is lower energy dissipation and lower stiffness degradation. A limitation to the model is that it doesn't simulate the initial friction between the mud and the timber frame. It appears that this limitation is more pronounced in the full-scale tests than the half-scale tests. This may be due to the fact that there was more shrinkage of the mud infill in the half-scale tests due to a

higher clay content, and hence less contact between the timber and the mud. Additionally, in the half-scale racking tests, an initial stabilising lateral load was applied which may have further reduced this initial bond.

The numerical model of the historic quincha frame is shown in Figure 46 and compared to the experimental test results obtained by Vicente and Torrealva (2013) shown in Figure 45. In the model, separation between the infill and the posts has occurred at the top and along the posts matching the cracking observed in the tests. Figure 47 compares the cyclic curves for the model and the tests. Aside from the species and age of the timber, there are several geometrical differences between the Replica Frame A and the historic frame. The original frame is taller at 4.5m, compared to 4m for the replica frame. Although both frames are the same width, the replica frame has one additional internal post meaning that the post spacing is greater. Furthermore, the original quincha wall has much longer top tenons, which was shown to be a substantial factor in increasing the lateral stiffness of the frame. Due to these variations, the original quincha frame is stiffer than the replica walls, and has a much larger reduction in stiffness in the second cycle than for the replica frame.

Figure 47 shows that the model does not match the initial stiffness of experimental test, as the stiffness for the first cycle in the experimental test is around three times that shown by the model. Despite this, the ultimate stiffness is matched well, with the experimental test giving a stiffness of only 3.9% greater than the model for the 100mm displacement cycles, which is the case in both directions. The reduction in stiffness in subsequent cycles, and energy dissipation is underestimated by the model, indicating that it cannot fully represent degradation of the frame.

This is because the constitutive material of the infill does not include a softening branch, which is a limitation of the available material library in the software.

Frame B

Figure 48 and Figure 49 show the deformed shapes at the 50 mm cycle for frame B for the experimental specimen and model respectively. Figure 50 compares the cyclic curves where a positive displacement represents a compressive deformation of the diagonal.

Table 5 compares the displacements obtained from the model with those of the test for different lateral forces. When the diagonal is in tension, the model has good agreement with the experimental results at a displacement of 50mm and 100mm. After this, the model overestimates the stiffness of the frame and does not show as much degradation as the tests. However, when diagonal is in compression, the model underestimates the stiffness of the frame, giving a lateral displacement of 52% greater than measured in the test. Since the model is run in force control, while the experimental tests were displacement controlled, the reduction in capacity in subsequent cycles will not be observed, however, there is a clear reduction in stiffness for the second cycle.

The major issue with the numerical model of Frame B is the greater influence that the diagonal has on the lateral stiffness of the frame. The reason for this is the way in which the internal post to diagonal brace connections are modelled. During the tests, the nails may loosen or detach, but it is difficult to model both continuity of the diagonal, and the ability of the nails to loosen, or

detach during the course of the cyclic loading. This is particularly apparent in the models of the PUCP test specimens since the diagonal passes over an additional internal post.

Summary of Results of Numerical Models

Overall, the numerical models show a good agreement with the experimental results, in the majority of cases being within a range of 20% error in terms of lateral displacement, lateral load, and vertical uplift of the tenon. However, it is apparent from the results of the cyclic tests that the model does not show the stiffness degradation observed in the tests, which may be improved with further investigations. Nonetheless, the numerical models are judged to give reasonable results that they may be used to develop a global model which will give a reasonably good indication to the behaviour of the building. Therefore, the following section describes the simplification of the model to reduce the run time for application to a case study building.

Simplification of the Model & Application to the Hotel Comercio

As shown in section 7.2, the in-plane behaviour of the numerical model has a high degree of agreement with experimental results. However, even a small section of a representative wall of the Hotel Comercio has a large number of contact elements, making the model cumbersome to run. Therefore, it is necessary to simplify the model without losing the correlation with the actual structural behaviour. To identify where simplifications can be made, a detailed model of one façade of the building was developed, which includes all contact elements. A sensitivity analysis

can then be carried out to determine which modifications can be made without dramatically affecting the behaviour. The overall lateral deflection is compared, as are the axial and bending stresses in the timber elements, and the levels of stress within the infill. A quantitative comparison of the deflected shape is also performed. This was done for a whole length of second storey on the shorter façade, as seen in Figure 1, to ensure that the windows and doors were considered.

First, the possibility of removing all contact elements, and assuming continuity between the frame and the infill was investigated. The results of this are shown in Figure 51 and compared with the results of the model under the same loading conditions with contact elements included, Figure 52. The comparison shows clearly that the continuity assumption substantially over estimates the lateral stiffness of the wall since almost no deformation is observed in Figure 51. Additionally, the axial stresses in the struts are significantly lower for the continuity assumption since a greater portion of the lateral load is taken by the infill. Therefore, full continuity is not considered to be a viable option. A second option is to reduce the number of contact elements by removing any contact elements which are inactive throughout the cyclic loading. From Figure 53 it can be seen that the area at the top of the infill is not in contact, as well as the areas adjacent to the openings. This remains the case in both in-plane directions. Since this was the case at all time-steps of the analysis, these elements can be removed. Additionally, the need for using a nonlinear truss element to simulate the lift up of the tenons from the mortice was investigated. It can be seen from Figure 54 that in most cases these elements are in tension indicating that the posts are moving upwards and showing that the inclusion of the nonlinear truss element to simulate this effect is essential.

Conclusions

This paper has described the methodology taken to develop numerical models of two quincha configurations found in a historic adobe-quincha building in Lima, Peru. The process of developing a robust numerical model of the quincha panels is challenging because of the complexity of the interaction between the infill and the timber frame and the nonlinear behaviour of the connections. Moreover a thorough calibration is hampered by the lack of reliable data on the mechanical characteristics of the mud and cane infill. However, it has been shown that the iterative process, where numerical modelling has been carried out in conjunction with targeted testing has shown to be an efficient and cost effective way of developing the assessment procedure.

A relatively high degree of complexity is required to achieve realistic results with the inclusion of nonlinear elements to model connections, infill, and contact between the infill and posts. In comparing the experimental and numerical outputs, the following issues emerge. Generally, the numerical models show good agreement with the tests, with the stiffness and capacity being within an error margin of 3% maximum when considering monotonic loading beyond the elastic behaviour. However when considering cyclic behaviour, then successful numerical strategies can be used to keep the margin of error within the target 20% in most cases. This is due to insufficient stiffness degradation in the model for successive cycles, when compared to the experimental results due to the constitutive model available in the software. Where the diagonal strut dominates the shear behaviour, rather than the infill, the model is more successful, signifying that the major difficulty is in modelling mud and cane infill. However, despite these

difficulties, a model of quincha can be developed that sufficiently reproduces the in-plane behaviour for use in a global model of a historic adobe-quincha building.

References

1995-1-1, BS EN. 2006. Eurocode 5: Design of timber structures – Part 1-1: General – Common rules and rules for buildings.

Aguilar, R., D. Torrealva, L.F. Ramos, and P.B. Lourenço. 2012. "Operational Modal Analysis Tests on Peruvian Historical Buildings: The Case Study of the 19th Century Hotel Comercio." 15th World Conference on Earthquake Engineering, Lisbon.

Aguilar, Rafael, Luís F Ramos, D Torrealva, and C Chácara. 2013. "Experimental modal identification of an existent earthen residential building." Proceedings of the 5th International Operational Modal Analysis Conference (IOMAC 2013). Guimarães.

Ali, Qaisar, Tom Schacher, Mohammad Ashraf, Bashir Alam, Akhtar Naeem, Naveed Ahmad, and Muhammad Umar. 2012. "In-Plane Behavior of the Dhajji-Dewari Structural System (Wooden Braced Frame with Masonry Infill)." Earthquake Spectra 28 (3):835-858. doi: 10.1193/1.4000051.

Autodesk (2013) Autodesk Simulation Multiphysics 2013 [Computer software]

Barrionuevo, R. 2011. "Investigación tecnológica aplicada: Domocaña." Informes de la Construcción 63 (523):51-58.

Bergman, Richard, Cai Zhiyong, Charlie G Carll, Carol A Clausen, Mark A Dietenberger, Robert H Flak, Charles R Frihart, Samuel V Glass, Christopher G Hunt, Rebecca E Ibach, David

E Kretschmann, Douglas R Rammer, and Robert J Ross. 2010. Wood Handbook, Wood as an Engineering Material. Edited by Forest Products Laboratory. Madison, WI.

Blondet, M., and J. Vargas. 1978. Investigaciones sobre vivienda rural. Lima, Peru: Ministerio de Transportes, Comunicaciones, Vivienda y Construcción / Pontificia Universidad Católica del Perú.

BSI. 2001. BS EN 12512: 2001 Timber Structures. Test methods. Cyclic testing of joints made with mechanical fasteners. BSI.

BSI. 2011. BS EN 594:2011 Timber structures. Test methods. Racking strength and stiffness of timber frame wall panels. BSI

Camilloni, Humberto Rodriguez. 2003. "Quincha architecture: The development of an antiseismic structural system in seventeenth century Lima." First International Congress on Construction History, Madrid.

Cancino, C., S. MacDonald, S. Lardinois, D. D'Ayala, D. Torrealva, C. F. Ferreira, and E. Vicente. 2012. "The Seismic Retrofitting Project: methodology for seismic retrofitting of historic earthen sites after the 2007 earthquake." The XIth International Conference on the Study and Conservation of Earthen Architecture Heritage, Lima, Peru.

Cancino, Claudia, and Sara Lardinois. 2012. Seismic Retrofitting Project: Assessment of Prototype Buildings. Los Angeles: The Getty Conservation Institute.

Cardoso, Rafaela, Mário Lopes, and Rita Bento. 2005. "Seismic evaluation of old masonry buildings. Part I: Method description and application to a case-study." Engineering Structures 27 (14):2024-2035. doi: http://dx.doi.org/10.1016/j.engstruct.2005.06.012.

Ceccotti, Ario, Paolo Faccio, Monica Nart, Carmen Sandhaas, and Paolo Simeone. 2006. "Seismic Behaviour of the Historic Timber-Frame Buildings in the Italian Dolomites." ICOMOS International Wood Committee 15th International Symposium.

Chrysostomou, CZ, P Gergely, and JF Abel. 2002. "A six-strut model for nonlinear dynamic analysis of steel infilled frames." International Journal of Structural Stability and Dynamics 2 (03):335-353.

Cuadra, C., C. Zavala, A. Abe, T. Saito, and S. Sugano. 2011. "Vibration Characteristics of Traditional Adobe-Quincha Buildings Located at Lima Historic Centre." 8th Conference on Urban Earthquake Engineering, Tokyo, Japan.

Custodio, Manuel Chavesta, Moisés Acevedo Mallque, and José Carlos Cano Delgado. 2012. Estudio Anatómico e Identificación de Especies Forestales. Evaluacion Estructural y Especificaciones Técnicas de las Maderas del Hotel El Comercio, Centro de Lima. Centro de Producción Forestal – Universidad Nacional Agraria La Molina (UNALM).

D143-94, ASTM. 2007. Standard Test Methods for Small Clear Specimens of Timber. West Conshohocken, PA: ASTM International.

D'Ayala, D., J. Worth, and O. Riddle. 2009. "Realistic shear capacity assessment of infill frames: Comparison of two numerical procedures." Engineering Structures 31 (8):1745-1761. doi: http://dx.doi.org/10.1016/j.engstruct.2009.02.044.

Descamps, T., J. Lambion, and D. Laplume. 2006. "Timber Structures: Rotational stiffness of carpentry joints." 9th World Conference on Timber Engineering, Portland, OR, August 6-10, 2006.

Doudoumis, I. N., J. Deligiannidou, and A. Kelesi. 2005. "Analytical modelling of masonry-infilled timber truss-works." 5th GRACM International Congress on Computational Mechanics, Limassol, 29 June - 1 July.

Doudoumis, Ionnis N. 2010. "Analytical Modelling of Traditional Composite Timber-Masonry Walls." Advanced Materials Research 133 - 134:441-446. doi: 10.4028/www.scientific.net/AMR.133-134.441.

Drdacky, M. F., F. Wald, and J. Mares. 1999. "Modelling of real historic timber joints." In Structural Studies, Repairs and Maintenance of Historical Buildings Vi, edited by C. A. Brebbia and W. Jager, 169-178. Southampton: Wit Press.

Ellul, Frederick, and Dina D'Ayala. 2012. "Realistic FE models to enable push-over non linear analysis of masonry infilled frames." Integration 10 (1):1.

Ferreira, J. G., M. J. Teixeira, A. Duţu, F. A. Branco, and A. M. Gonçalves. 2014. "Experimental Evaluation and Numerical Modelling of Timber-Framed Walls." Experimental Techniques 38 (4):45-53. doi: 10.1111/j.1747-1567.2012.00820.x.

Ghavami, Khosrow, and Albanise B Marinho. 2005. "Propriedades físicas e mecânicas do colmo inteiro do bambu da espécie do bambu da espécie Guadua angustifolia Guadua angustifolia." Revista Brasileira de Engenharia Agrícola e Ambiental 9 (1):107-114.

González, G., and J. Gutiérrez. 2005. "Structural performance of bamboo 'bahareque' walls under cyclic load." Journal of Bamboo and Rattan 4 (4):353-368. doi: 10.1163/156915905775008345.

Groenenberg, R. J. 2010. "Adobe Structures in Earthquake Zones." MSc, Faculty of Civil Engineering & Geosciences Structural Engineering, Delft University of Technology Pontificía Universidad Católica del Perú.

Hicyilmaz, K. M. O., T. Wilcock, C. Izat, J. da-Silva, and R. Langenbach. 2012. "Seismic Performance of Dhajji Dewari." 15th World Conference on Earthquake Engineering, Lisbon.

IRMA, Information Resources Management Association. 2013. Sustainable Practices: Concepts, Methodologies, Tools and Applications: IGI Global.

Karakostas, Christos, Vassilios Lekidis, Triantafyllos Makarios, Thomas Salonikios, Issam Sous, and Milton Demosthenous. 2005. "Seismic response of structures and infrastructure facilities during the Lefkada, Greece earthquake of 14/8/2003." Engineering Structures 27 (2):213-227. doi: 10.1016/j.engstruct.2004.09.009.

Komatsu, Kohei, Akihisa Kitamori, Kiho Jung, and Takuro Mori. 2009. "Estimation of The Mechanical Properties of Mud Shear Walls Subjecting to Lateral Shear Force." 11th International Conference on Non-conventional Materials and Technologies (NOCMAT 2009), Bath, UK, 6-9 September 2009.

Kouris, Leonidas Alexandros S., and Andreas J. Kappos. 2012. "Detailed and simplified non-linear models for timber-framed masonry structures." Journal of Cultural Heritage 13 (1):47-58. doi: http://dx.doi.org/10.1016/j.culher.2011.05.009.

Lamb, George N. 1947. The mahogany book. 6th ed. Chicago: Mahogany Association. Available: https://archive.org/details/mahogany00lamb

Mackerle, Jaroslav. 2005. "Finite element analyses in wood research: a bibliography." Wood Science and Technology 39 (7):579-600. doi: 10.1007/s00226-005-0026-9.

Makarios, Triantafyllos, and Milton Demosthenous. 2006. "Seismic response of traditional buildings of Lefkas Island, Greece." Engineering Structures 28 (2):264-278. doi: 10.1016/j.engstruct.2005.08.002.

Meier, Eric. 2014. "The Wood Database." Accessed 23 February. http://www.wood-database.com/.

Miranda, O., J. Gallardo, C. Cuadra, and J. Ogawa. 2000. "Reduction of seismic damage in Peruvian traditional constructions." International Conference on computer simulation in risk analysis and hazard mitigation No. 2., Bologna, Italy.

Pang, WeiChiang, and Masood H Shirazi. 2010. "Next generation numerical model for nonlinear in-plane analysis of wood-frame shear walls." World conference on timber engineering, Riva del Garda, Italy, June 20–24; 2010.

Paredes, Lourdes Ana Maria Cardenas. 2008. "Analisis de Vulnerabilidad Estructural del Hotel Comercio." Proyecto de thesis para obtar el titulo profesional de ingeniero civil, Facultad de Ingenieria, Universidad Ricardo Palma.

Poletti, Elisa, Graça Vasconcelos, and Daniel V Oliveira. 2013. "Influence of infill on the cyclic behaviour of traditional half-timbered walls." International conference on rehabilitation and restoration of structures, Chennai, India; 2013.

Quinn, N., D. D'Ayala, and D. Moore. 2012. "Experimental testing and numerical analysis of quincha under lateral loading." Structural Analysis of Historic Constructions, Wroclaw, Poland.

Quinn, Natalie, and Dina D'Ayala. 2014. "In-Plane Experimental Testing on Historic Quincha Walls." 9th International Conference on Structural Analysis of Historical Constructions, Mexico City.

Ramos, Luis F., and Paulo B. Lourenço. 2004. "Modeling and vulnerability of historical city centers in seismic areas: a case study in Lisbon." Engineering Structures 26 (9):1295-1310. doi: 10.1016/j.engstruct.2004.04.008.

Ramskill, Thomas Edward. 2002. "Effect of Cracking on Lag Bolt Performance." PhD, Civil Engineering, Virginia Tech.

Rojas-Bravo, Julio, and Carlos Fernandez Baca. 2012. "Case Study of Repairing an Adobe Colonial Building in Cusco, Peru." 8th Alexander von Humboldt International Conference: Natural Disasters, Global Change and the Preservation of World Heritage Sites, Cusco, Peru, 12-16 November 2012.

Ruíz, Nicola Tarque, Guido Camata, Enrico Spacone, Humberto Varum, and Marcial Blondet. 2013. "Non-linear dynamic analysis of a full-scale unreinforced adobe model." Earthquake Spectra 30(4) 1643-1661

SENCICO. 2006. Ensayos sobre simulacion sismica en dos modulos de adobe y quincha de 2 pisos. Servicio Nacional de Capacitación para la Industria de la Construcción.

Sparkes, A. J. 1968. The strength of mortise and tenon joints. Maxwell Road Stevenage Hertfordshire: Furniture Industry Res. Assoc.

Tarque, Nicola. 2008. "Seismic Risk Assessment of Adobe Dwellings." Masters Degree in Earthquake Engineering and Enginering Seismology, Universita delgi Studi di Pavia.

Tavera, Hernando, Isabel Bernal, FleurO Strasser, MariaC Arango-Gaviria, JohnE Alarcón, and JulianJ Bommer. 2009. "Ground motions observed during the 15 August 2007 Pisco, Peru, earthquake." Bulletin of Earthquake Engineering 7 (1):71-111. doi: 10.1007/s10518-008-9083-4.

Torrealva, Daniel, and Alejandro Muñoz. 1987. Proyecto de Investigación "Vivienda de Quincha en dos Pisos" Primera Etapa: Comportamiento Dinamico. Lima: Pontificía Universidad Catolica del Perú.

Torrealva, Daniel, and Erika Vicente. 2012. "Experimental Evaluation of Seismic Behaviour of Quincha Walls from the Historical Centre of Lima, Peru." 15th World Conference on Earthquake Engineering, Lisbon.

Torrealva, Daniel and Vicente, Erika. 2013. Personal Communication: "Information on Original Quincha Wall Tests." 10/06/2013.

Tsai, Pin-Hui, and Dina D'Ayala. 2011. "Performance-based seismic assessment method for Taiwanese historic Dieh-Dou timber structures." Earthquake Engineering & Structural Dynamics 40 (7):709-729. doi: 10.1002/eqe.1050.

Tsakanika - Theohari, Eleftheria, and Harris Mouzakis. 2010. "A post-byzantine mansion in Athens. The restoration project of the timber structural elements." World conference on timber engineering, Riva del Garda, Italy, June 20–24; 2010.

Vargas, Julio. and Ottazzi, Gianfranco. 1981. Investigaciones en adobe: Pontificia Universidad Católica del Perú, Departamento de Ingeniería.

Vargas, Julio. 1981. "Adobe Testing. Basis for a Seismic Resistant Code." Conference Proceedings

Vicente, Erika, and Torrealva, Daniel. 2014. "Mechanical properties of adobe masonry of historical buildings in Peru." 9th International Conference on Structural Analysis of Historic Constructions, Mexico City.

Wald, F., J. Mares, Z. Sokol, and M. Drdacky. 2000. "Component Method for Historical Timber Joints." In NATO Science Series: II. Mathematics, Physics and Chemistry 4, 417-424.

Walker, Charles F. 2008. Shaky Colonialism: The 1746 Earthquake-Tsunami in Lima, Peru, and Its Long Aftermath: Duke University Press.

Wilkinson, Thomas Lee. 1971. "Theoretical lateral resistance of nailed joints." Journal of the Structural Division 97 (5):1381-1398.

		Experimental Observations	Conclusions for Numerical Model
(A and B)	Pull-out of tenons	Tenons at bottom pull out of mortices. No vertical movement measured for top tenons	The model needs to allow for vertical uplift at the base of the posts. Vertical movement does not need to be considered for top tenons.
	Rotation of tenons	If tenons unable to rotate, the stiffness of the frame is overestimated	Model needs to allow for semi-rigid rotational behaviour of the mortice and tenon joint.
(FRAME A and B)	Contribution of infill to stiffness and capacity	Infill increases stiffness by more than 4 times for both frames, and doubles ultimate lateral strength capacity.	The mechanical characteristics used for the infill in the model should be calibrated from this data (see 5.2).

	Effect of the infill on the deformed shape	The overall response of the frame is fundamentally different when infill present and relies on infill shear stiffness and contact between infill and frame.	Infill should be modelled using shell elements rather than alternative of using a spring or brace to model contribution of infill to strength stiffness. The latter would give different deformed shape and misleading failure mechanism.
(FRAME A ONLY)	Connection between citara struts and frame	Negligible rotation occurs and no pull out occurs at the joint of the diagonal citara with frame's post and beam.	Citara struts modelled as continuous with frame elements for direct action and shear but released in rotation.
	Contribution of adobe blocks to behaviour	Adobe blocks undamaged. The citara prevents rotation of bottom tenons.	Not necessary to include adobe blocks in model, simply accounting for their weight. Rotation of bottom tenons prevented.
(FRAM	Compression	Frame stiffer in	Buckling capacity of diagonal needs to

	of diagonal brace	compression than tension but buckling of diagonal occurred	be considered.
	Diagonal connection to post	Failure at the connection. No rotation measured, but diagonal moved axially when nails yielded.	Connection modelled using nonlinear axial spring. Stiffness and capacity of spring calculated depending on geometrical and material characteristics of particular joint
	Connections to internal posts	Relative rotation was observed between the diagonal and posts	End-releases inserted between diagonal and posts in model to allow relative rotation

Mechanical Characteristics (Average Values)	**Sapele**		**Spanish Cedar**	**True Mahogany**	**Cypress**	
	Test values from samples extracted from HC (Custodio, Mallque, and Delgado 2012)	Reference values for specimens free of defect (Bergman et al. 2010, Meier 2014)	Reference value for specimen free of defect (Bergman et al. 2010, Meier 2014)	Reference value for specimen free of defect (Bergman et al. 2010, Meier 2014)	Test values from samples extracted from HC (Custodio, Mallque, and Delgado 2012)	Reference value for specimen free of defect (Mexican Cypress) (Bergman et al. 2010, Meier 2014)
Density (kg/m^3)	490	490-670	470	480-833	470	512 - 515

Modulus of elasticity (GPa) (static bending)	7.7	12.0 – 12.5	9.1 – 9.9	10.1 – 10.3	5.4	7.0 - 9.9
Modulus of rupture (MPa)	60.3	105.5-109.9	70.8 - 79.3	79.3 – 80.8	47.9	71.0 - 73.1
Compressive strength parallel to grain (MPa)	32.7	56.3	42.8	50.6	31.1	37.1
Shear parallel to grain (MPa)	6.2	15.6	7.6	11.2	7.6	10.9
Compressive strength perpendicular to grain (MPa)	4.6	-	-	-	4.3	-

Material	**Parameter**	**Value**	**Source**
Timber: **2 species both modelled as isotropic material using MoE values** ***Isotropic***	Density (kg/m^3)	*Caoba Africana:*400 *Cypress:*390	Experimental tests on samples extracted from HC (Custodio, Mallque, and Delgado 2012)
	Poisson ratio	0.3	(Bergman et al. 2010)
	Elastic Modulus in Bending (GPa)	*Caoba Africana:*7.7 *Cypress:*6.4	Experimental tests on samples extracted from HC (Custodio, Mallque, and Delgado 2012)
Adobe masonry ***Isotropic***	Density (kg/m^3)	1600	(IRMA 2013)
	Poisson ratio	0.2	(Groenenberg 2010)
	Elastic Modulus (MPa)	225	(Vicente and Torrealva 2014)

Horizontal canes ***Isotropic***	Density (kg/m^3)	710	(Barrionuevo 2011)
	Poisson ratio	0.26	Taken from tests on bamboo specimens (Ghavami and Marinho 2005)
	Elastic Modulus in Bending (GPa)	18.0	Obtained experimentally on similar size canes
Infill of mud and canes ***Von Mises with isotropic hardening***	Density (kg/m^3)	1160	Obtained experimentally
	Poisson ratio	0.2	Taken to be same as adobe
	Elastic Modulus (MPa)	200	Numerically calibrated from experimental tests of Frame A with and without infill.
	Yield Strength (MPa)	0.05	
	Strain hardening modulus (MPa)	0.3	
Contact between	Contact modulus	*Frame*	Calculated from k=AE/L where

infill and timber frame ***Contact elements***	(compression) (kN/m)	*A:*47,500 *Frame B:*51,350 (These values are included for reference but are mesh sensitive and depend on the size of the post)	A is area of contact, E is elastic modulus of timber perpendicular to the grain and L is the length of the contact element.

Frame A Replica	Lateral Displacement (mm)	Lateral Load (kN)		Percentage Error
		Experimental	Numerical	
Cycle 1	50	6.20	5.53	12%
	-50	-5.95	-6.80	-13%
Cycle 2	50	4.53	4.93	-8%
	-50	-5.35	-6.53	-18%
Cycle 1	100	7.10	8.17	-13%
	-100	-6.75	-8.98	-25%
Cycle 2	100	5.26	7.31	-28%
	-100	-5.69	-6.66	-15%

		Lateral Displacement (mm)		
Frame B Replica	**Lateral Force (kN)**	**Experimental**	**Numerical**	**Percentage Error**
Cycle 1	10	24.25	20.40	19%
Cycle 1	-10	-29.30	-60.76	-52%
Cycle 2	12	50.14	43.14	16%
Cycle 2	-12	-93.74	-99.18	-5%

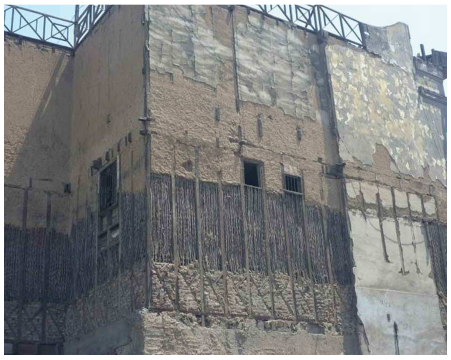

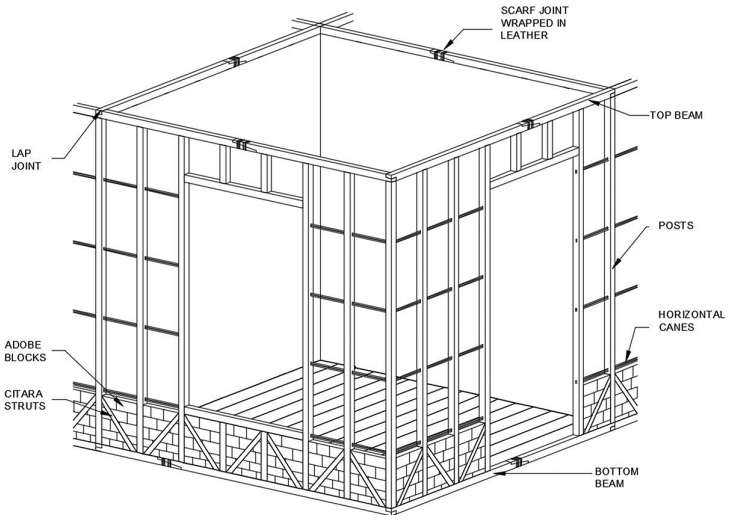

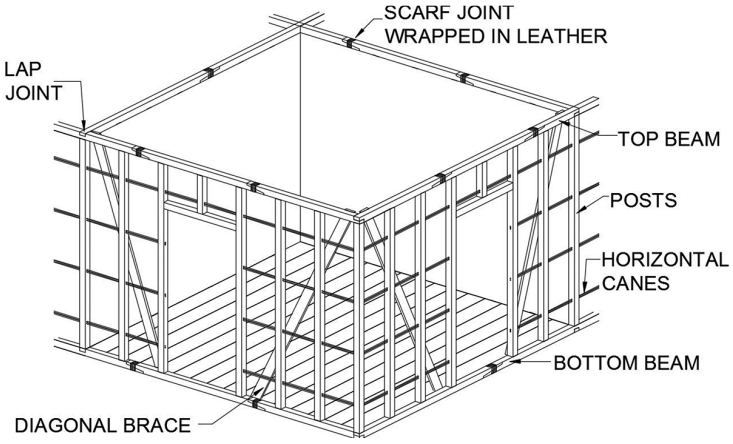

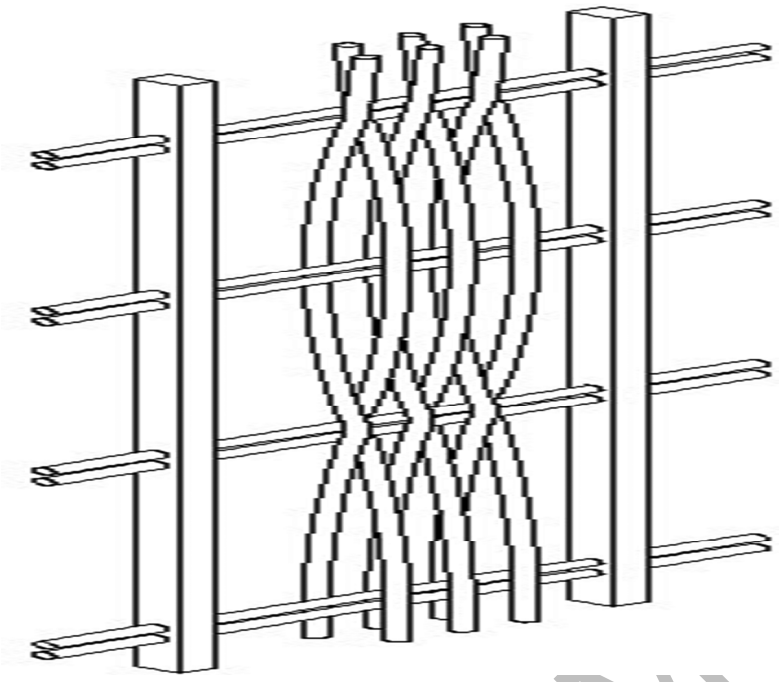

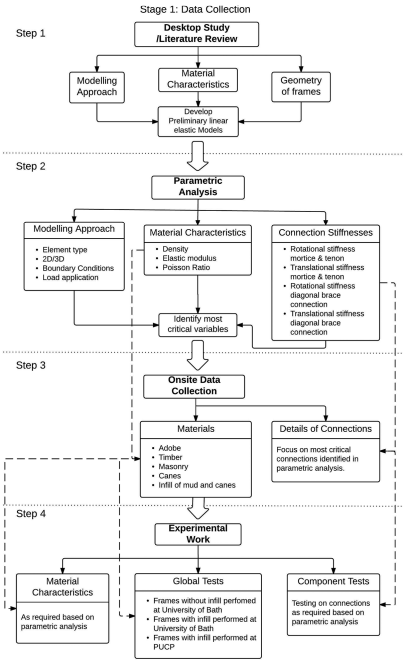

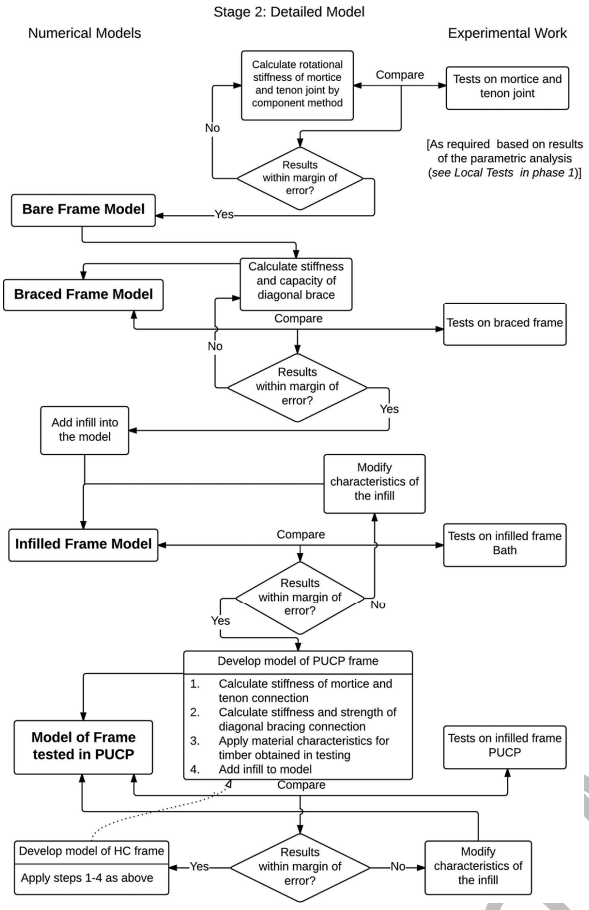

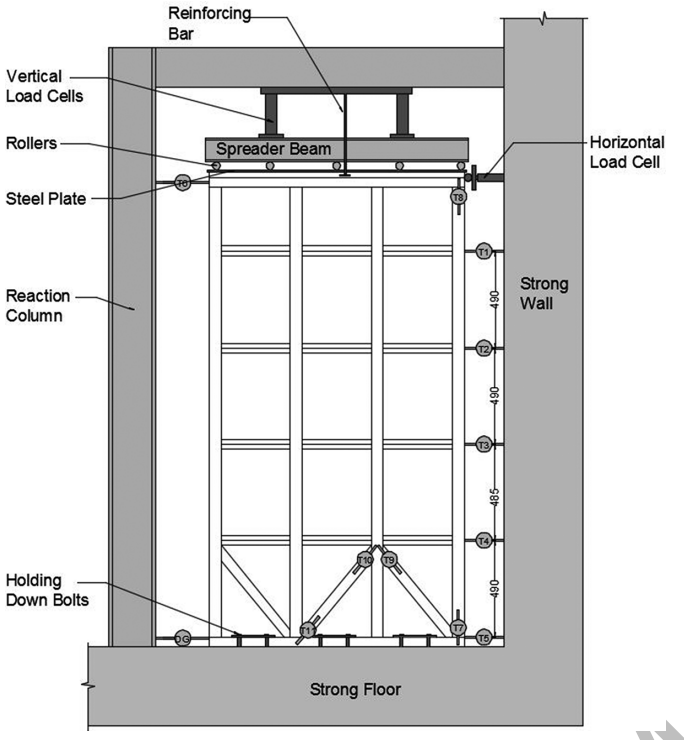

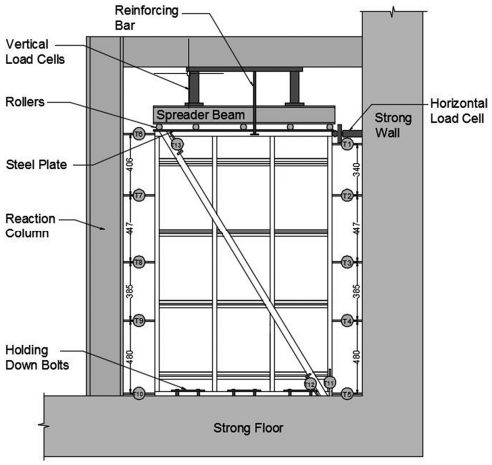

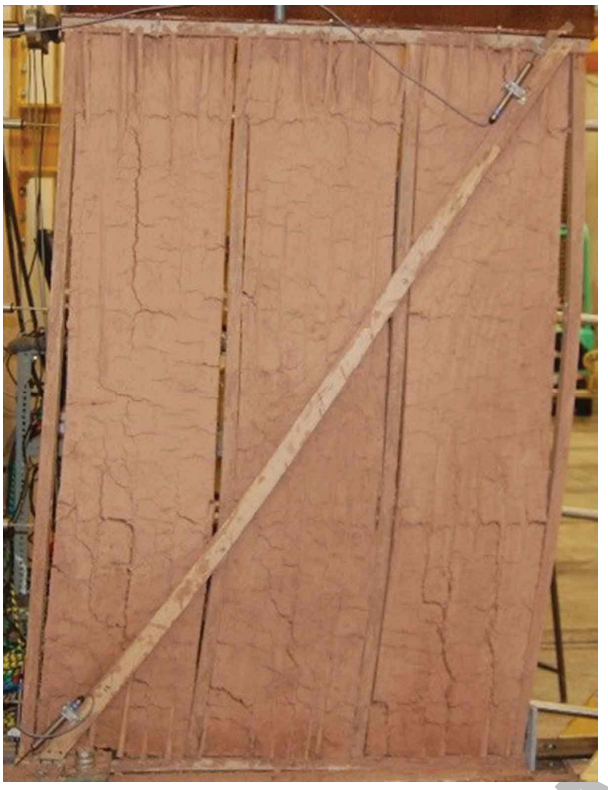

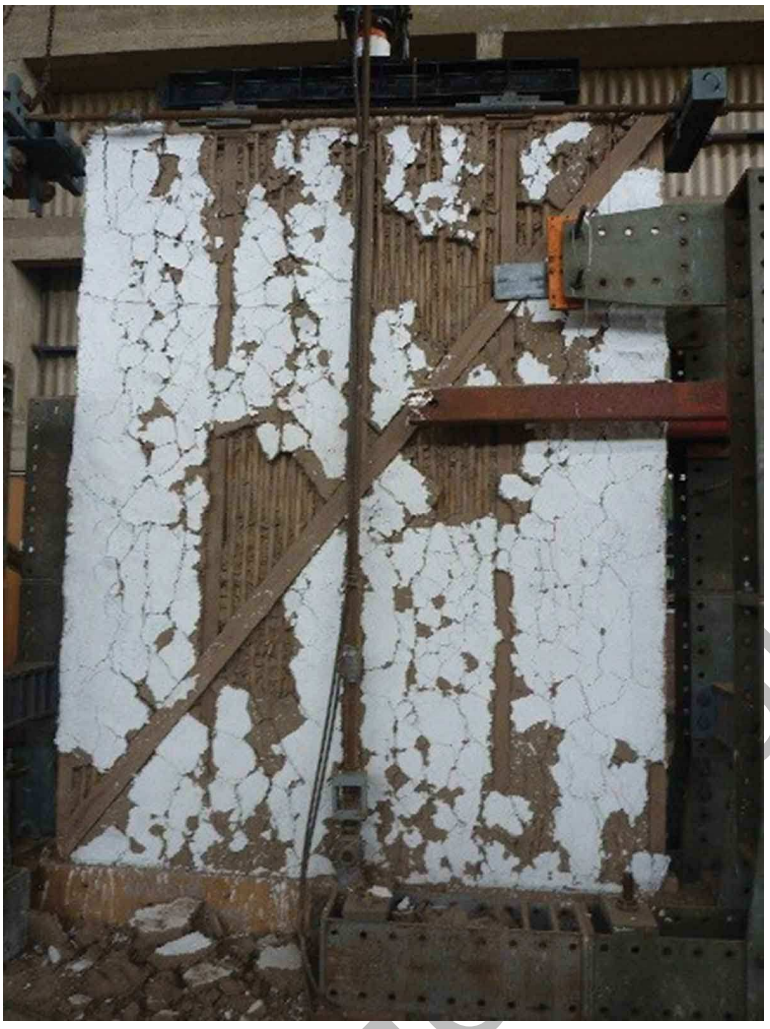

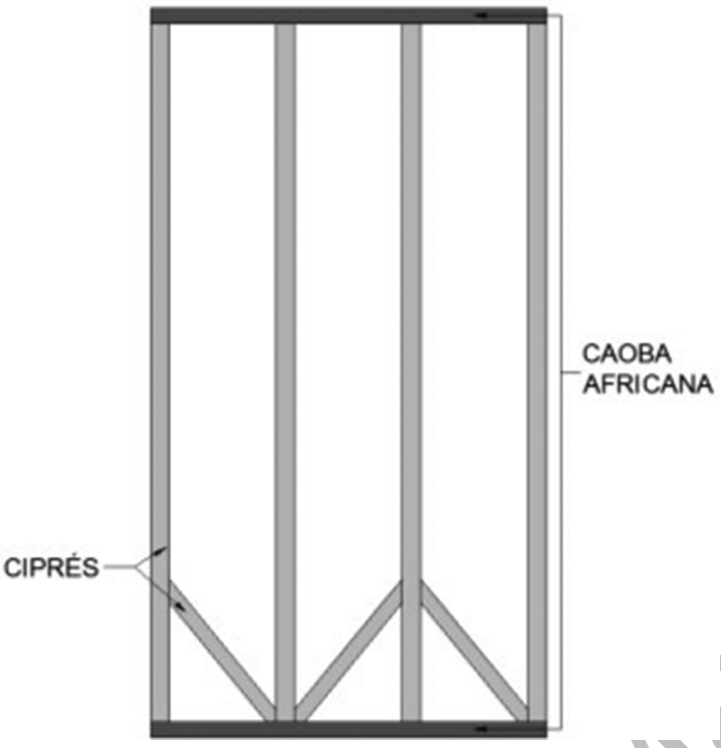

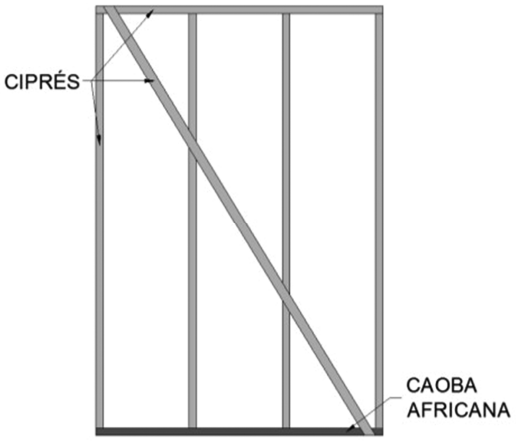

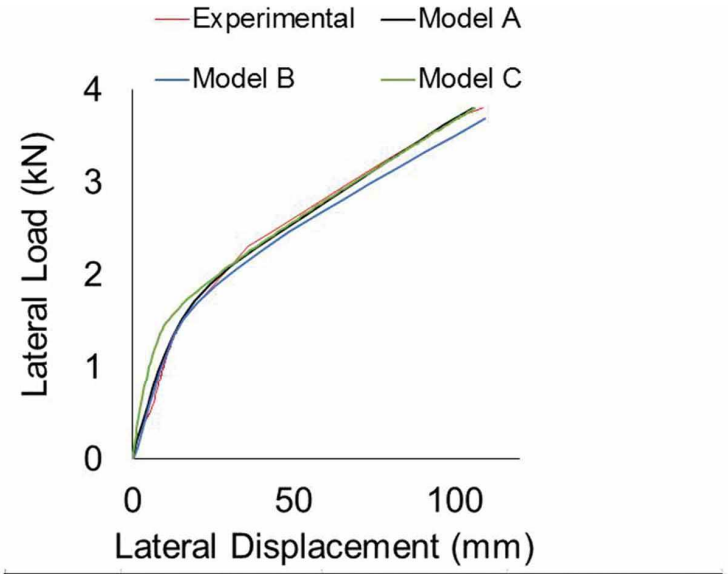

	Elastic Modulus (MPa)	Yield Strength (MPa)	Strain Hardening Modulus (MPa)
Model A	200	0.05	0.3
Model B	200	0.05	0.15
Model C	500	0.05	0.3